



DE GRUYTER
OPEN

GEOCHRONOMETRIA 45
DOI 10.1515/geochr-2015-0092

Available online at
<http://www.degruyter.com/view/j/geochr>



ASSESSING THE MAXIMUM LIMIT OF SAR-OSL DATING USING QUARTZ OF DIFFERENT GRAIN SIZES

SUPPLEMENTARY MATERIALS

VALENTINA ANECHITEI-DEACU^{1,2}, ALIDA TIMAR-GABOR^{1,2}, DANIELA CONSTANTIN²,
OANA TRANDAFIR-ANTOHI^{2,3}, LAURA DEL VALLE⁴, JOAN J FORNÓS⁴,
LLUÍS GÓMEZ-PUJOL⁴ and ANN G. WINTLE^{5,6}

¹*Faculty of Environmental Sciences and Engineering, Babeş-Bolyai University, Cluj-Napoca, Romania*

²*Interdisciplinary Research Institute on Bio-Nano-Sciences, Babeş-Bolyai University, Cluj-Napoca, Romania*

³*Faculty of Physics, Babeş-Bolyai University, Cluj-Napoca, Romania*

⁴*Earth Sciences (Geology and Paleontology “Guillem Colom”) Research Group, Department of Biology,
Universitat de les Illes Balears, Palma, Spain*

⁵*Institute of Geography and Earth Sciences, Aberystwyth University, Aberystwyth, UK*

⁶*McDonald Institute for Archaeological Research, University of Cambridge, Cambridge, UK*

Corresponding author: A. Timar-Gabor
e-mail: alida.timar@ubbcluj.ro

ISSN 1897-1695 (online), 1733-8387 (print)

© 2018 V. Anechitei-Deacu *et al.* This work is licensed under the Creative Commons Attribution-NonCommercial-NoDerivatives 3.0 License.

1. SUPPLEMENTARY TEXTS

Text S1

To test the thermal stability of the OSL signal measured from 0 to 0.308 s, annealing curves were constructed, increasing the 10 s preheat in steps of 10°C. A cutheat to 180°C has been used. The results for the 63–90 µm and 4–11 µm of sample M#6# are very similar to each other and to the results for the calibration quartz (**Fig. S3**). The first order derivative of the curves (inset to **Fig. S3**) shows the origin of the fast OSL signals for the 4–11 µm and 63–90 µm quartz from sample M#6# to be linked to a trap which has its maximum rate of emptying at a temperature of at least 300°C. To further evaluate the thermal stability of the OSL signal for quartz from these samples, an isothermal luminescence decay experiment was carried out for sample M#11# (63–90 µm), as described in a recent study by our group (Timar-Gabor *et al.*, 2017). The time evolution of the OSL signal at a given temperature and the lifetime dependency on temperature are shown in **Fig. S4a** and **S4b**, respectively. The Arrhenius parameters obtained ($E = 1.66 \pm 0.05$, $\log_{10}s = 13.2 \pm 0.5$) fall in the range of other studies (Timar-Gabor *et al.*, 2017) and are indistinguishable from those of the main trap identified in a former study (Murray and Wintle, 1999). Our results show a trap lifetime of about 69 Ma at 20°C, thus indicating that thermal instability is not an issue for quartz extracted from these samples and that the signal should be stable enough to date the last 1 Ma.

Text S2

For those aliquots of fine quartz from sample M#6# given 50, 100, 200, 300, 400, 500, 1000, 1500, 1800 and 2500 Gy in addition to their natural dose, growth curves were constructed using the SAR protocol and these are given in **Fig. S5**. For the 63–90 µm fraction of sample M#11#, SAR dose response curves were constructed for all aliquots given laboratory doses (50, 200, 500 and 1000 Gy) in addition to their natural dose (**Fig. S6**). Values of D_e obtained for the natural plus added doses for both fine and coarse quartz are given in **Table S2**. The ratio of these values to the total dose is plotted as a function of the total dose in **Fig. S7a** and **S7b** for fine and coarse quartz, respectively. The measured values for the fine fraction for added doses of 50, 100 and 200 Gy (equivalent to natural doses of 225, 275 and 375 Gy, respectively) are underestimated by 9%, but for larger added doses the underestimation increases to 50% for 2500 Gy (**Table S2** and **Fig. S7a**). With regard to the coarse quartz, the value measured for 50 Gy added to the natural dose (equivalent to a natural dose of 157 Gy) is underestimated by 6%, but the underestimation increases to 60% for 1000 Gy (**Table S2** and **Fig. S7b**). All doses given within the dose recovery test for the coarse quartz from sample M#11# were measured as unknown by the SAR protocol and the recovered doses as well as the

ratios between these and the given doses are presented in **Table S3**; the dose recovery ratios are graphically represented as function of dose in **Fig. S8**. As expected, these results are very similar to those obtained for the same sample when doses are added to the natural. This data is not available for the fine quartz fraction of sample M#6#.

Text S3

The D_e values measured for the Chinese loess sample (XF 153) when doses are added to the natural dose for both fine and coarse quartz, as well as the ratio of these values to the total doses are given in **Table S7** and graphically represented in **Fig. S9**. An underestimation of ~10% of the values is observed even for added doses as low as 70 Gy for fine and 26 Gy for coarse quartz (equivalent to natural doses of 350 Gy). The values measured for fine and coarse quartz from the same sample when doses are given within the dose recovery test are presented in **Table S8** alongside the ratios between these values and the given doses. For both quartz fractions the SAR protocol can accurately recover the given doses up to 500 Gy (**Fig. S10a** and **S10b** for fine and coarse quartz, respectively).

2. SUPPLEMENTARY FIGURES

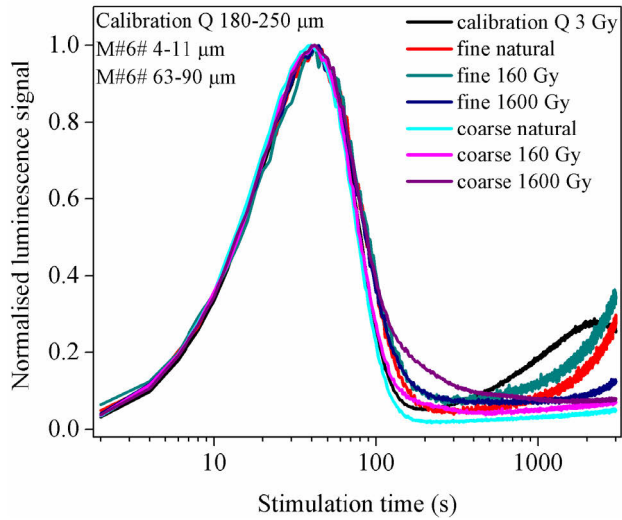


Fig. S1. LM-OSL of natural and regenerated signals for one aliquot of fine (4–11 μm) and coarse (63–90 μm) quartz extracted from sample M#6# in comparison to the signal for 180–250 μm calibration quartz. Stimulation was performed at 125°C by ramping the stimulation power from 0–80% in 3000 s after a preheat at 220°C for 10 s. One data channel represents 2 seconds of stimulation. For a better visual comparison, each curve was normalized to its maximum value. Natural and regenerated LM-OSL signals for both fractions show the peak maximum early in the curve and overlap the signal observed for calibration quartz.

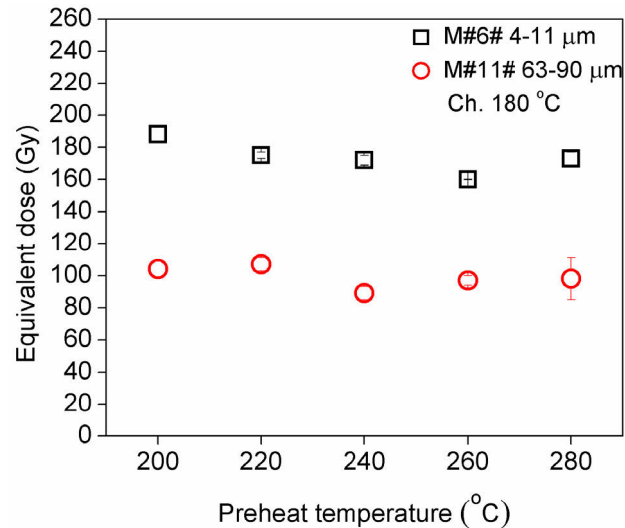


Fig. S2. Preheat plateau test results for fine (4–11 μm) and coarse (6–90 μm) quartz fractions from samples M#6# and M#11#, respectively.

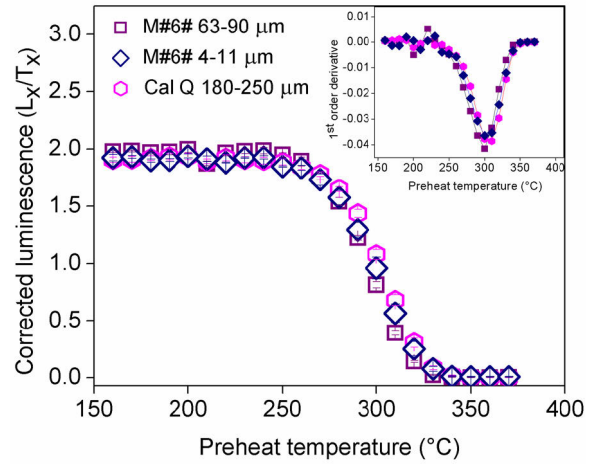


Fig. S3. Pulse annealing curves for OSL signals for fine (4–11 μm) and coarse (63–90 μm) quartz grains for sample M#6# compared with that for coarse (180–250 μm) calibration quartz. Each data set is the average of three aliquots. The inset presents the first order derivatives of the data. The regenerative dose for both fine and coarse grains of sample M#6# was 32 Gy and a test dose of 16 Gy was used. For calibration quartz a regenerative dose of 8 Gy in combination with a test dose of 4 Gy was used. The error bars often fall within the data point on the graph.

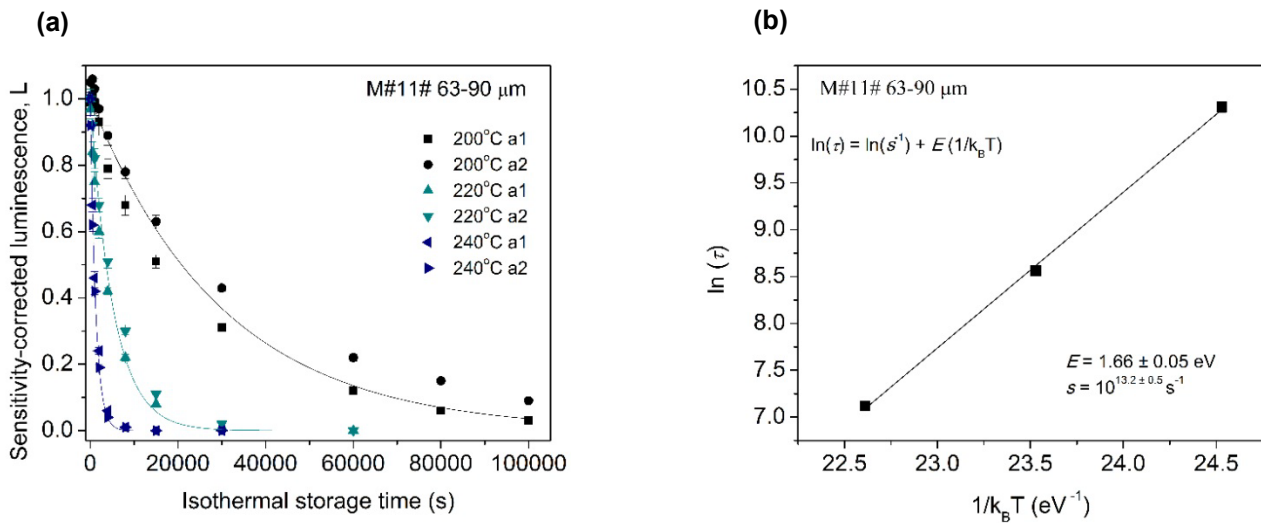


Fig. S4. (a) Isothermal decay of the coarse (63–90 μm) quartz OSL signal over 28 hours for sample M#11#. Two aliquots were used for each holding temperature and the averaged values were used for fitting. The solid lines are best fits of a single decaying exponential function. (b) Mean lifetimes, τ , derived from the data in Fig. S4a are plotted against $1/k_B T$. The solid line is the best fit of $\tau = s^{-1} \exp(E/k_B T)$, where E and s are the trap depth and frequency factor, respectively.

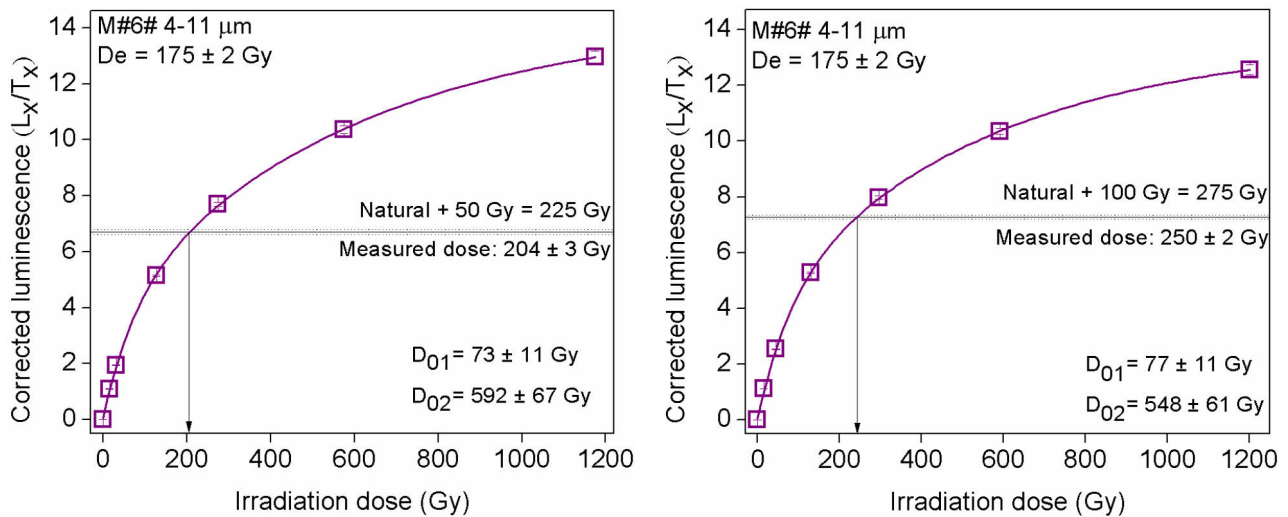


Fig. S5. (Continuation on the next page)

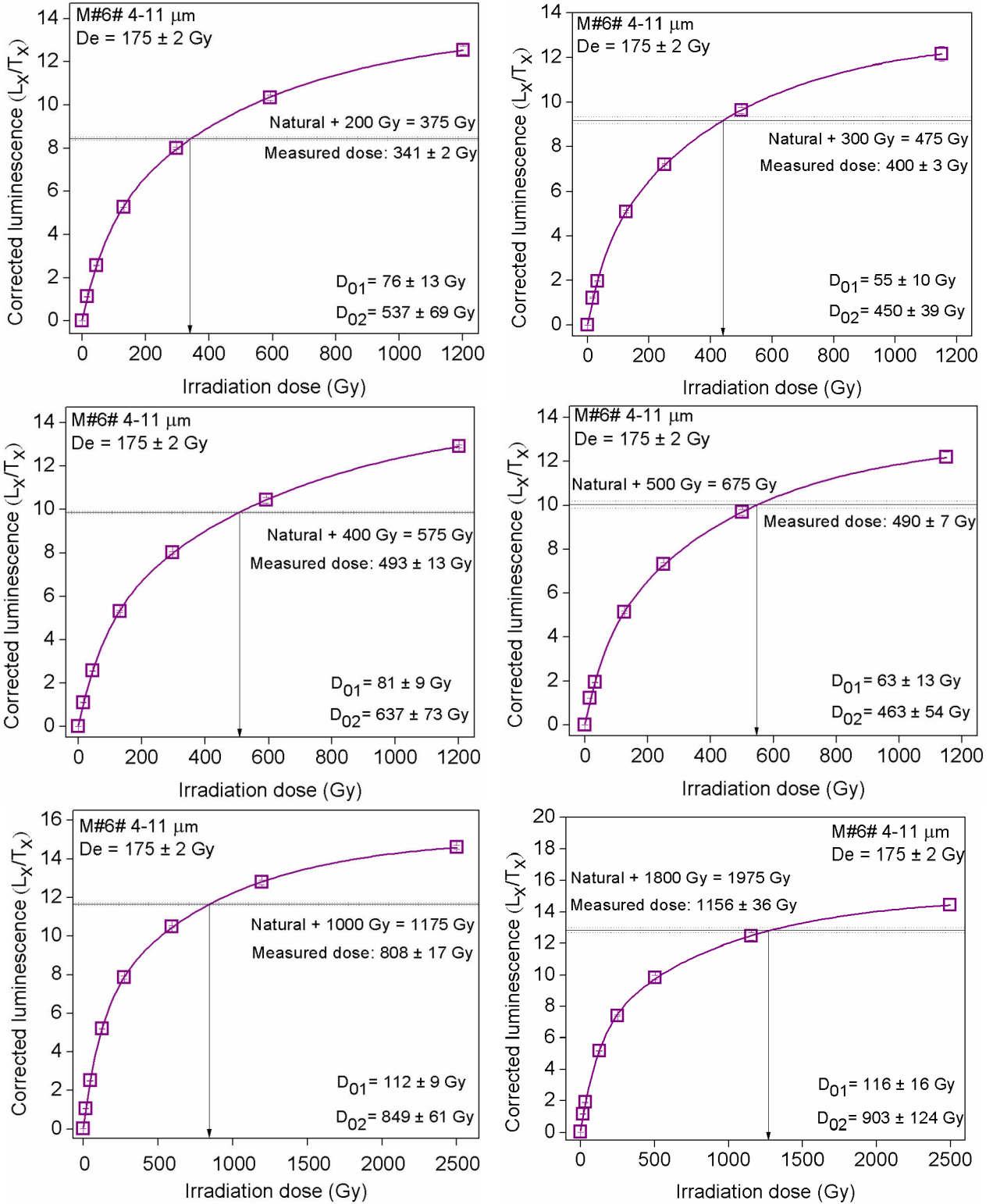


Fig. S5. (Continuation on the next page)

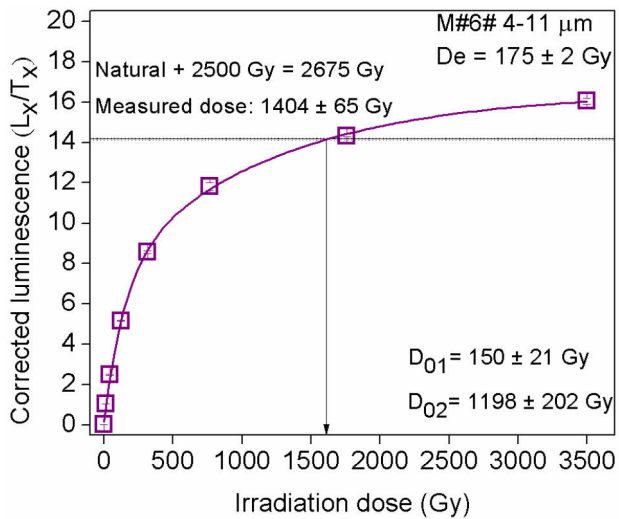


Fig. S5. Average dose-response curves constructed after adding different doses on top of the natural signals for 4–11 μm quartz from sample M#6#. Each growth curve was constructed using three aliquots. The sensitivity corrected signal corresponding to the sum of natural and added dose is interpolated on the constructed growth curve. Please note that the error bars fall within the data points.

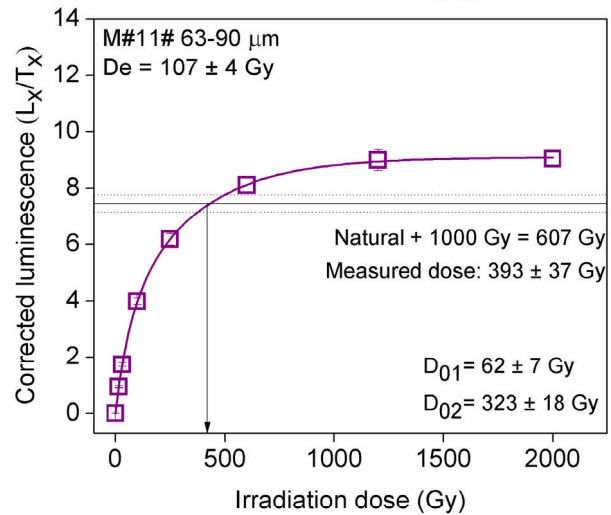
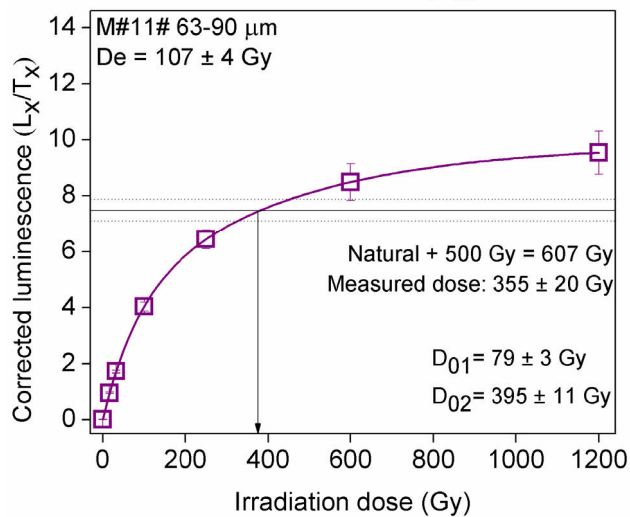
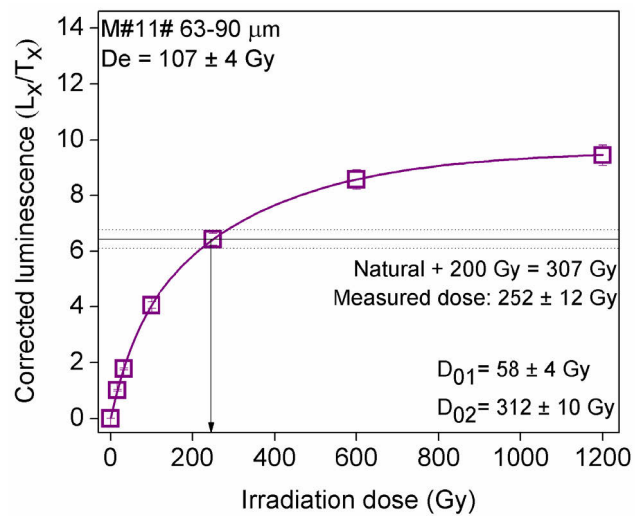
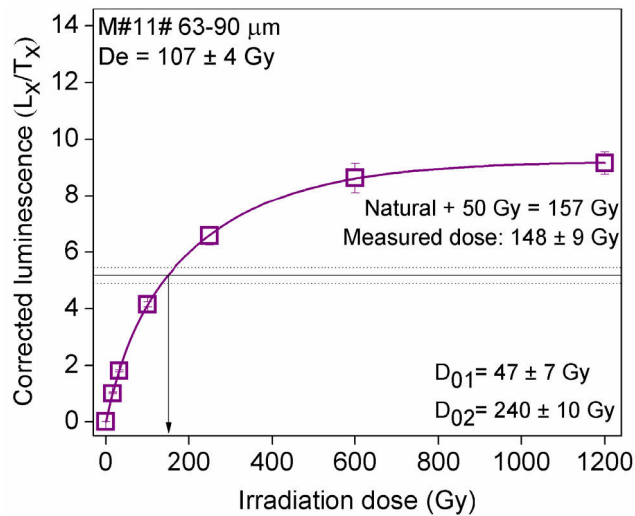


Fig. S6. Average dose-response curves constructed after adding different doses on top of the natural signals for 63–90 μm quartz from sample M#11#. Each growth curve was constructed using between three and seven aliquots. The sensitivity corrected signal corresponding to the sum of natural and added dose is interpolated on the constructed growth curve. Please note that some of the error bars fall within the data points.

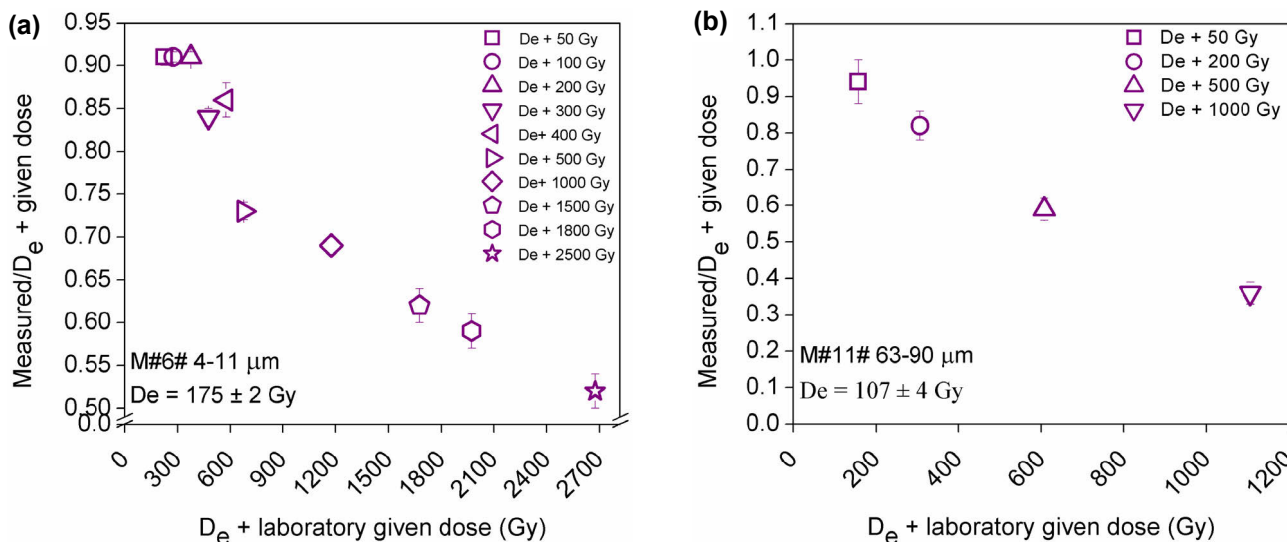


Fig. S7. Ratios between the measured dose and the known dose (natural+added dose) as a function of the latter for (a) fine quartz from sample M#6# and (b) coarse quartz from sample M#11#.

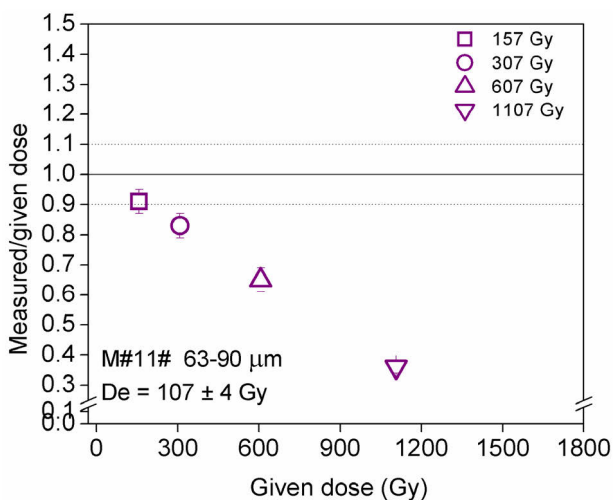


Fig. S8. Ratios between the measured dose and the dose given within the dose recovery test as a function of the latter for coarse quartz from sample M#11#.

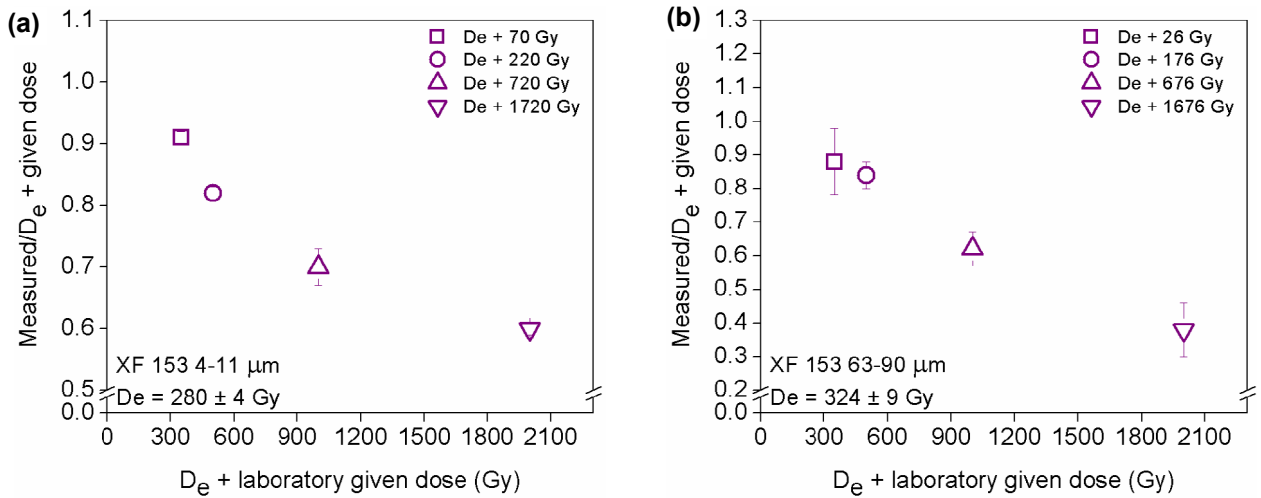


Fig. S9. Ratios between the measured dose and the known dose (natural+added dose) as a function of the latter for (a) fine quartz and (b) coarse quartz from sample XF 153.

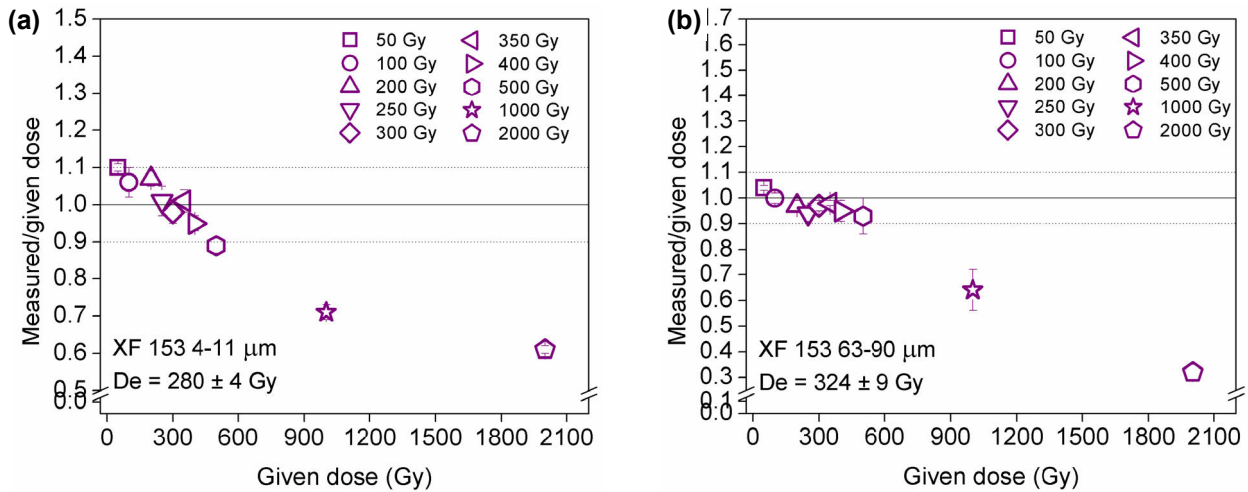


Fig. S10. Ratios between the measured dose and the dose given within the dose recovery test as a function of the latter for (a) fine quartz and (b) coarse quartz from sample XF 153.

3. SUPPLEMENTARY TABLES

Table S1. Values of D_{01} and D_{02} obtained from the data in Fig 6, obtained when using doses up to progressively higher doses. n represents the number of data points used to construct the dose-response curves.

The maximum dose up to which the laboratory growth curve was constructed (Gy)	D_{01} (Gy)	D_{02} (Gy)
575 _{n=11}	46 ± 8	315 ± 25
675 _{n=12}	66 ± 13	433 ± 78
1175 _{n=13}	81 ± 9	565 ± 47
1675 _{n=14}	97 ± 11	704 ± 64
1975 _{n=15}	112 ± 12	849 ± 93
2675 _{n=16}	135 ± 11	1149 ± 126
4000 _{n=17}	147 ± 10	1361 ± 100
6000 _{n=18}	156 ± 10	1527 ± 88

Table S2. Values of D_e obtained on 4–11 μm (sample M#6#) and 63–90 μm (sample M#11#) quartz for natural and added doses, as well as the ratio of these values to the sum of the natural and added dose. n denotes the number of accepted aliquots.

D_e + Laboratory given dose (Gy)	Measured dose (D_e +given dose) (Gy)	Measured/ D_e +given dose
4–11 μm (sample M#6#)		
$D_e = 175 \pm 2$ Gy		
D_e +50 = 225	204 ± 3 _{n=3}	0.91 ± 0.01
D_e +100 = 275	250 ± 2 _{n=3}	0.91 ± 0.01
D_e +200 = 375	341 ± 2 _{n=3}	0.91 ± 0.01
D_e +300 = 475	400 ± 3 _{n=2}	0.84 ± 0.01
D_e +400 = 575	493 ± 13 _{n=3}	0.86 ± 0.02
D_e +500 = 675	490 ± 7 _{n=3}	0.73 ± 0.01
D_e +1000 = 1175	808 ± 17 _{n=3}	0.69 ± 0.01
D_e +1500 = 1675	1034 ± 35 _{n=3}	0.62 ± 0.02
D_e +1800 = 1975	1156 ± 36 _{n=3}	0.59 ± 0.02
D_e +2500 = 2675	1404 ± 63 _{n=3}	0.52 ± 0.02
63–90 μm (sample M#11#)		
$D_e = 107 \pm 4$ Gy		
D_e +50 = 157	148 ± 9 _{n=4}	0.94 ± 0.06
D_e +200 = 307	252 ± 12 _{n=5}	0.82 ± 0.04
D_e +500 = 607	355 ± 20 _{n=4}	0.59 ± 0.03
D_e +1000 = 1107	393 ± 37 _{n=4}	0.36 ± 0.03

Table S3. Doses recovered within the dose recovery test for 63–90 μm quartz from sample M#11# as well as the ratio of these values to the given dose. n denotes the number of accepted aliquots.

Given dose (Gy)	Measured dose (Gy)	Measured/given dose
157	143 ± 6 _{n=5}	0.91 ± 0.04
307	255 ± 12 _{n=7}	0.83 ± 0.04
607	396 ± 27 _{n=2}	0.65 ± 0.04
1107	395 ± 19 _{n=3}	0.36 ± 0.02

Table S4. Average values for L_n^*/T_n^* measured for natural plus added dose, L_r/T_r measured after one bleach as in dose recovery test and L_x/T_x measured in a SAR sequence for fine (sample M#6#) and coarse quartz (sample M#11#). For an easier approach, the ratios $(L_n^*/T_n^*)/(L_x/T_x)$ and $(L_r/T_r)/(L_x/T_x)$ are also given.

D_e (175 ± 2 Gy) + given dose (Gy)	L_n^*/T_n^*	L_n^*/T_n^* error	Given Dose (Gy)	L_x/T_x	L_x/T_x error	L_r/T_r	L_r/T_r error	$(L_n^*/T_n^*)/(L_x/T_x)$	$(L_n^*/T_n^*)/(L_x/T_x)$ error	$(L_r/T_r)/(L_x/T_x)$	$(L_r/T_r)/(L_x/T_x)$ error
4–11 μm (sample M#6#) $D_e = 175 \pm 2$ Gy											
D_e+50	6.71	0.09	225	7.10	0.02	-	-	0.95	0.01		
D_e+100	7.28	0.07	275	7.81	0.06	7.99	0.07	0.93	0.01	1.02	0.01
D_e+200	8.44	0.07	375	9.00	0.05	-	-	0.94	0.01		
D_e+300	9.19	0.15	475	9.87	0.08	9.21	0.15	0.93	0.01	0.93	0.02
D_e+400	9.86	0.05	575	10.53	0.10	-	-	0.94	0.01		
D_e+500	10.03	0.16	675	11.31	0.11	10.33	0.22	0.89	0.02	0.91	0.02
D_e+1000	11.66	0.07	1175	13.23	0.16	12.30	0.10	0.88	0.01	0.93	0.01
D_e+1500	12.83	0.14	1675	14.40	0.25	12.32	0.47	0.89	0.02	0.86	0.04
D_e+1800	12.84	0.17	1975	14.80	0.21	13.25	0.18	0.87	0.02	0.90	0.02
D_e+2500	14.17	0.05	2675	15.59	0.27	14.37	0.21	0.91	0.02	0.92	0.02
D_e+3825	14.06	0.08	4000	16.46	0.34	14.20	0.50	0.85	0.02	0.86	0.04
D_e+5825	14.67	0.16	6000	17.00	0.42	14.09	0.37	0.86	0.02	0.83	0.03
63–90 μm (sample M#11#) $D_e = 107 \pm 4$ Gy											
D_e+50	5.18	0.28	157	4.78	0.13	5.05	0.17	1.08	0.07	1.06	0.05
D_e+200	6.44	0.32	307	6.19	0.19	6.46	0.38	1.04	0.06	1.04	0.07
D_e+500	7.48	0.39	607	7.24	0.30	7.55	0.43	1.03	0.07	1.04	0.07
D_e+1000	7.46	0.31	1107	7.86	0.37	7.55	0.56	0.95	0.06	0.96	0.08

Table S5. Average values for L_n^*/T_n^* measured for natural plus added dose and L_x/T_x measured in corresponding SAR sequences for fine and coarse quartz for sample XF 153. For an easier approach, the ratios $(L_n^*/T_n^*)/(L_x/T_x)$ and $(L_r/T_r)/(L_x/T_x)$ are also given.

D_e + given dose (Gy)	L_n^*/T_n^*	L_n^*/T_n^* error	Given Dose (Gy)	L_x/T_x	L_x/T_x error	$(L_n^*/T_n^*)/(L_x/T_x)$	$(L_n^*/T_n^*)/(L_x/T_x)$ Error
4–11 μm (sample XF 153) $D_e = 280 \pm 4$ Gy							
D_e+70	8.24	0.14	350	8.60	0.09	0.96	0.02
D_e+220	9.14	0.12	500	9.73	0.05	0.94	0.01
D_e+720	11.14	0.17	1000	12.13	0.15	0.92	0.02
D_e+1720	13.04	0.30	2000	14.41	0.20	0.90	0.02
63–90 μm (sample XF 153) $D_e = 324 \pm 9$ Gy							
D_e+26	6.00	0.13	350	6.17	0.09	0.97	0.03
D_e+176	7.01	0.30	500	6.57	0.11	1.07	0.05
D_e+676	7.21	0.28	1000	7.25	0.19	0.99	0.05
D_e+1676	7.58	0.08	2000	7.32	0.35	1.04	0.05

Table S6. Average values for L_r/T_r measured after one bleach as in dose recovery test and L_x/T_x measured in corresponding SAR sequences for fine and coarse quartz for sample XF 153. For an easier approach, the ratios $(L_n^*/T_n^*)/(L_x/T_x)$ and $(L_r/T_r)/(L_x/T_x)$ are also given.

Given dose (Gy)	L_r/T_r	L_r/T_r error	Given Dose (regenerative point, Gy)	L_x/T_x	L_x/T_x error	$(L_r/T_r)/L_x/T_x$	$(L_r/T_r)/L_x/T_x$ error
4–11 μm (sample XF 153) $D_e = 280 \pm 4$ Gy							
50	2.95	0.03	50	2.73	0.03	1.08	0.01
100	4.63	0.13	100	4.48	0.01	1.03	0.03
200	6.88	0.03	200	6.62	0.10	1.04	0.02
250	7.56	0.07	250	7.56	0.02	1.00	0.01
300	7.97	0.14	300	8.02	0.08	0.99	0.02
350	8.75	0.16	350	8.60	0.09	1.02	0.02
400	9.17	0.10	400	9.35	0.02	0.98	0.01
500	9.61	0.04	500	9.73	0.05	0.99	0.01
1000	11.24	0.11	1000	12.13	0.15	0.93	0.01
2000	13.17	0.07	2000	14.41	0.20	0.91	0.01
63–90 μm (sample XF 153) $D_e = 324 \pm 9$ Gy							
50	2.75	0.03	50	2.68	0.04	1.02	0.02
100	3.96	0.05	100	3.97	0.08	1.00	0.02
200	5.32	0.15	200	5.39	0.16	0.99	0.04
250	5.50	0.20	250	5.61	0.20	0.98	0.05
300	5.69	0.10	300	5.73	0.12	0.99	0.03
350	6.11	0.15	350	6.17	0.09	0.99	0.03
400	6.44	0.08	400	6.51	0.08	0.99	0.02
500	6.49	0.11	500	6.57	0.11	0.99	0.02
1000	6.70	0.13	1000	7.25	0.19	0.92	0.03
2000	6.46	0.08	2000	7.32	0.35	0.88	0.04

Table S7. Values of D_e obtained on 4–11 μm and 63–90 μm quartz from sample XF 153 for natural and added doses, as well as the ratio of these values to the sum of the natural and added dose. n denotes the number of accepted aliquots.

D_e + Laboratory given dose (Gy)	Measured dose (D_e +given dose) (Gy)	Measured/ D_e +given dose
4–11 μm (sample XF 153) $D_e = 280 \pm 4$ Gy		
$D_e+70 = 350$	$318 \pm 2_{n=4}$	0.91 ± 0.01
$D_e+220 = 500$	$411 \pm 6_{n=4}$	0.82 ± 0.01
$D_e+720 = 1000$	$700 \pm 26_{n=4}$	0.70 ± 0.03
$D_e+1720 = 2000$	$1204 \pm 10_{n=3}$	0.60 ± 0.01
63–90 μm (sample XF 153) $D_e = 324 \pm 9$ Gy		
$D_e+26 = 350$	$307 \pm 34_{n=4}$	0.88 ± 0.10
$D_e+176 = 500$	$419 \pm 34_{n=4}$	0.84 ± 0.04
$D_e+676 = 1000$	$621 \pm 50_{n=4}$	0.62 ± 0.05
$D_e+1676 = 2000$	$762 \pm 154_{n=2}$	0.38 ± 0.08

Table S8. Doses recovered within the dose recovery test for 4–11 μm and 63–90 μm quartz from sample XF 153 as well as the ratio of these values to the given dose. n denotes the number of accepted aliquots.

Given dose (Gy)	Measured dose (Gy)	Measured/given dose
4–11 μm (sample XF 153) $D_e = 280 \pm 4$ Gy		
50	$55 \pm 1_{n=3}$	1.10 ± 0.01
100	$106 \pm 8_{n=3}$	1.06 ± 0.04
200	$215 \pm 7_{n=3}$	1.07 ± 0.02
250	$253 \pm 19_{n=3}$	1.01 ± 0.04
300	$294 \pm 17_{n=3}$	0.98 ± 0.03
350	$354 \pm 19_{n=3}$	1.01 ± 0.03
400	$379 \pm 13_{n=3}$	0.95 ± 0.02
500	$445 \pm 16_{n=3}$	0.89 ± 0.02
1000	$709 \pm 40_{n=3}$	0.71 ± 0.02
2000	$1218 \pm 40_{n=3}$	0.61 ± 0.01
63–90 μm (sample XF 153) $D_e = 324 \pm 9$ Gy		
50	$52 \pm 1_{n=4}$	1.04 ± 0.01
100	$100 \pm 4_{n=4}$	1.00 ± 0.02
200	$193 \pm 6_{n=4}$	0.97 ± 0.02
250	$234 \pm 14_{n=4}$	0.94 ± 0.03
300	$290 \pm 11_{n=4}$	0.97 ± 0.02
350	$343 \pm 10_{n=4}$	0.98 ± 0.01
400	$379 \pm 28_{n=4}$	0.95 ± 0.04
500	$466 \pm 70_{n=4}$	0.93 ± 0.07
1000	$636 \pm 131_{n=3}$	0.64 ± 0.08
2000	$647 \pm 89_{n=2}$	0.32 ± 0.03

REFERENCES

- Murray AS and Wintle AG, 1999. Isothermal decay of optically stimulated luminescence in quartz. *Radiation Measurements* 32(4–5): 57–73, DOI [10.1016/S1350-4487\(98\)00097-3](https://doi.org/10.1016/S1350-4487(98)00097-3).
- Timar-Gabor A, Buylaert J-P, Guralnik B, Trandafir-Antohei O, Constantin D, Anechitei-Deacu V, Jain M, Murray AS, Porat N, Hao Q and Wintle AG. On the importance of grain size in luminescence dating using quartz. *Radiation Measurements* 106: 464–471, DOI [10.1016/j.radmeas.2017.01.009](https://doi.org/10.1016/j.radmeas.2017.01.009).